



Sharif University of Technology  
**Scientia Iranica**  
*Transactions A: Civil Engineering*  
<http://scientiairanica.sharif.edu>



# Reliability-based approach to fragility analysis of lattice transmission tower in the type test

A. Mahmoudi<sup>a,b</sup>, M.A. Jafari<sup>b,\*</sup>, and K. Nasrollahzadeh<sup>a</sup>

a. *Department of Civil Engineering, K. N. Toosi University of Technology, Tehran, P.O. Box 15875-4416, Iran.*

b. *Department of Power Industry Structures Research, Niroo Research Institute (NRI), Tehran, P.O. Box 1466-5517, Iran.*

Received 16 May 2021; received in revised form 7 August 2021; accepted 22 November 2021

## KEYWORDS

Lattice transmission tower;  
 Type test;  
 Fragility curve;  
 Limit State Function (LSF);  
 Eccentricity of connections;  
 Reliability analysis;  
 Equal angle section.

**Abstract.** Precise prediction of the structural capacity of lattice transmission towers under different loads is essential to accurate assessment of the reliability of transmission networks. In doing so, the uncertainties inherent in the modeling parameters of the towers should be taken into account. In this regard, the present paper developed a probabilistic framework to analyze the failure of a 230 kV double-circuit tower in a full-scale type test accounting for the uncertainties including eccentricity at the connections, joint slippage, and initial imperfection in the members. Three loading patterns were applied to the manufactured full-scale tension tower. A finite element model of the tower was established and verified by the test results considering the mentioned uncertainties. The importance vectors derived from reliability analysis showed the effect of each of these parameters on the displacement of the target points as well as the maximum load-carrying capacity of towers' members for these load patterns. Further, additional moments resulting from eccentricity at the connections were highlighted through a proposed regression-based equation. The failure probability of the tested tower was then determined for different load factors whose results were presented in terms of fragility curves. Finally, the effect of eccentricity on the tower failure was quantified.

© 2022 Sharif University of Technology. All rights reserved.

## 1. Introduction

Most lattice towers are self-supporting equipped by members with equal angle sections connected by bolts. In many cases, these bolted joints cause eccentricity by transferring the load from the load location to the central longitudinal axis of the member. Tower designers have long concluded that the results of the ideal truss models cannot correspond well to those of tested towers. Prototype towers are often tested

for destruction to assess the extra margin of safety available beyond the factor of safety stipulated in the specifications. These tests also serve as a means of checking the quality of craft during manufacturing [1]. Rao et al. [2] compared the results derived from the failures of cross arms in four tested towers with those from nonlinear finite element analysis. They concluded that the load-carrying capacity of the towers depended on not only the load-carrying capacity of their members but also several other factors such as connection details, uncertainties of the members' eccentricities, and non-uniform distribution of forces in bolted connections and gusset plates. Tian et al. [3] performed full-scale tests of a latticed steel transmission tower. In the Finite Element Model (FEM), a buckling and softening failure model was developed to evaluate the behavioral patterns of the transmission tower. Shukla

\*. *Corresponding author. Tel.: +98 21 88079400-(4482); Fax: +98 21 88574768 E-mail addresses: amirmahmoodiaut@gmail.com (A. Mahmoudi); mjafari@nri.ac.ir (M.A. Jafari); nasrollahzadeh@kntu.ac.ir (K. Nasrollahzadeh)*

and Selvaraj [4] conducted full-scale testing of a 132 kV double-circuit suspension tower where the strain gauges were installed on some prominent members to calculate the actual load. They reported that the actual forces were slightly lower than the calculated values. Tian et al. [5] performed full-scale testing of a latticed steel tubular transmission tower with major emphasis on the failure mechanism of the tower under an extreme wind load. Rao et al. [6] presented different types of premature failures observed during full-scale testing and then, modeled them using finite element software. Lu et al. [7] proposed some experiments to model the force-displacement behavior of bolted connections to reinforce the existing towers by adding the auxiliary members. Albermani et al. [8] used a nonlinear methodology for structural failure prediction rather than forensic analysis. Their obtained results were confirmed through full-scale testing of a transmission tower that collapsed during the test. de Souza et al. [9] suggested some topology design recommendations, constructed 72 FEMs, and applied them to the same self-supporting 230 kV real structure with small differences in their elements' configurations. Jiang et al. [10] applied eccentricity to the model as a constant value, which was already calculated using working drawings. Albermani and Kitipornchai [11] reported that the main failure mode was buckling in the compressive legs where the plastic joints occurred in the simulation.

Jiang et al. [12] referred to the bolted connections as spring elements. In the spring method, bolted joints are replaced by spring elements to simulate pin or semi-rigid connections. Upon using spring elements, the models matched the experimental results and significantly reduced the modeling complexity [12]. Szafran and Rykaluk [13] examined two independent load conditions first by considering only the axial force and second, accounting for the axial force plus an additional bending moment due to the effect of eccentric connection. Yaghoobi and Shooshtari [14] presented eight different types of load-deformation curves of joints. An et al. [15] investigated the effect of deformations and bolt slip in bolted joints on the axial stiffness of the tower leg members. Ungkurapinan et al. [16] conducted laboratory studies to propose more accurate models of joint slippage. They developed empirical relations to evaluate joint slippage and force-displacement behaviors. Their slippage model was employed by Ahmed et al. [17] to study the behavior of transmission towers under working loads using the finite element method. Kitipornchai et al. [18] developed joint slippage models for conventional connections in transmission towers and demonstrated that although the joint slippage had a significant impact on the predicted displacements of the towers, it had a negligible effect on the analysis results of stresses and almost no

impact on the maximum predicted ultimate capacities of the lattice towers. Temple et al. [19] highlighted the effects of residual stress and initial imperfections on the ultimate behavior in mission towers in their numerical study. They concluded that the buckling failure of the main leg was the main failure mode caused by the P- $\Delta$  effect. In seismic collapse assessment of the Iranian code-conforming C.R.C. buildings, Hoseini et al. [20] quantified several uncertainties such as the P- $\Delta$  effect, deterioration in strength and stiffness, and cyclic deterioration in the structural components. Fong et al. [21] compared the loads of a test that caused failure in the member, with the values predicted by designing codes as well as the results of numerical analyses. According to their findings, consideration of the connection rigidity impact could increase the predicted ultimate loads compared to the model with the ideal pinned connections. Fu et al. [22] tested a full-scale 230 kV suspension tower. They developed the framework of a uniform imperfection mode method for the transmission tower to estimate the strength capacity and performed numerical validation by comparing it with a full-scale test.

Tian et al. [23] utilized the 1000 kV tower model using Tian-Ma-Qu model to assess the nonlinear axial behaviors (yielding and buckling). Da Silva et al. [24] compared the results from numerical models, experiments, and theoretical linear elastic truss analyses and concluded that the truss modeling method was limited in load cases, thus exhibiting considerable discrepancies in member forces. To obtain more accurate predictions of the responses of transmission towers through finite element analysis, Lee and McClure [25] developed a finite beam element for the equal angle section and predicted the ultimate capacity of the members considering eccentricity, boundary conditions, and nonlinear behaviors derived from geometry and materials. Prasad Rao and Kalyanaraman [26] developed a model considering members' eccentricities, local and rotational displacements of connections, and nonlinear behaviors of the utilized materials. They verified the final model using the test results for a more accurate estimation of the forces in the secondary braces of such structures. Zhuge et al. [27] modeled all equal angle members and bolts in 3D brick elements.

Fu and Li [28] considered the material properties and section dimension uncertainty in transmission towers based on the Latin Hypercube Sampling technique to establish uncertain FEMs. Mohammadi Darestani et al. [29] evaluated the impact of uncertainties on both demand and capacity as well as the impacts of different modeling complexities such as buckling, joint slippage, and joint failure on the extreme wind performance of transmission towers. Fu et al. [30] presented an analytical uncertainty method to estimate the strength capacity and predict the failure patterns

of transmission towers induced by wind and rain loads. Tessari et al. [31] applied the performance-based wind engineering methodology to the probabilistic analysis of steel towers. Upon using FORM, a sensitivity analysis was conducted to evaluate the effect of uncertainties such as the structural strength and wind-structure interaction on the structural response. Pan et al. [32] numerically studied the impacts of different sources of uncertainty on the fragility and seismic responses of transmission towers. Fu et al. [33] proposed an uncertainty analysis method for tower structures subjected to wind load. Sotoudeh et al. [34] applied Incremental Dynamic Analysis (IDA) method to four Limit State Functions (LSFs) in the seismic performance of the integrated dam reservoir FEM to estimate the fragility curve. Li et al. [35] obtained the failure probability of a single-circuit transmission tower-line system for either a structural component or entire structure LSFs considering the meteorological uncertainties. Liu et al. [36] discussed the structural LSFs using a new adaptive support vector regression method. They also verified the efficiency of this method where closed-form failure functions such as truss bridge structure were not available. Shafaei et al. [37] developed a procedure to increase the accuracy flashover rates by accurately modeling network components such as the transmission tower and chain of insulators based on Monte Carlo method. Szafran et al. [38] presented a reliability estimation procedure for steel lattice telecommunication towers based on tensioned joint reliability for a full-scale pushover test of a 40 m high lattice tower. Liu and Feng [39] proposed a new method based on the mechanical structure of the tower to calculate the reliability index of the 500 kV transmission tower structure. Szafran et al. [40] assessed the reliability of steel telecommunication tower using the Stochastic Finite Element Method (SFEM).

The modeling parameters including the initial imperfection of the members, joint slippage, and eccentricity at the connections are essentially uncertain; therefore, they should be treated as random variables in the structural modeling of the transmission towers. However, a very limited number of studies have been conducted on uncertainties of all of these parameters in the tower model. Instead, a majority of the published works have dealt with the modeling parameters in a fully deterministic way. At best, very few studies took only one variable as random while the others as deterministic values. However, the current study considered all of the above-mentioned connection related factors in the static pushover analysis of a lattice tower using OpenSees [41] and compared the obtained results with those from the measurements and observations of a sample tower type test, which was performed at the NRI-OSTS tower test station in Arak, Iran in 2008. More specifically, this study proposed a probabilistic

framework where the modeling parameters involved in the problem under study were regarded as random variables while determining the reliability indexes of both displacement-based as well as force-based LSFs for type test results of a tower under different load conditions including high wind, wind and ice, and broken wire. The relative importance vectors for the modeling variables were identified using the reliability techniques. Random variables were ranked based on their relative importance, thus helping the designer determine the degree of importance of these variables in the probabilistic analysis. In addition, it is possible to determine which variables and their uncertainty should be ignored in the probabilistic analysis. To this end, due to the high computational effort of the model, the importance of each of these variables considered in the model were quantitatively determined using First Order Second Moment (FOSM) analysis [42] based on the tower displacement of LSFs and the member forces. A great deal of attention was paid to the additional moments exerted by eccentricity at the connections considering a regression-based equation. The final outcome of this research regarding the fragility curves for the tested tower was presented, in which the failure probability of the tower in different load stages were correlated with the connection eccentricities.

## 2. Development and calibration of the FEM

### 2.1. Type test of a sample tower

Tower testing provides information on the support behavior under the load, fit-up verification, actions on the structure in deflected positions, adequacy of connections, and other benefits [1]. The type test results on a 230 kV, 90-degree tension, double-circuit, 47-meter high tower with a square base of 15.34 m×15.34 m were utilized in this study. The tower was constructed using St 52 (DIN 2391). Figure 1 presents the detailed configuration of the cross arms, neck, legs, and primary and secondary braces. The tested tower includes three cross arms, i.e., the top, median, and bottom cross arms. The displacements corresponding to every load pattern in each step of increasing loads at points A, B, C, and D, shown in Figure 1, were recorded using a theodolite.

The tower test station has a square testbed with sides of 20 m that can withstand the reaction forces of the tower bases up to 675 tons per base. Each tower base is connected to the testbed through a foundation interface suitable for tensile or compressive forces by special clamps designed for this particular application. Vertical, longitudinal, and transverse loads were applied using steel wires through eight electric winches of 5 and 10 tons at low speed. The winches can also move in reverse; hence, this set can be controlled directly from the control room in two modes

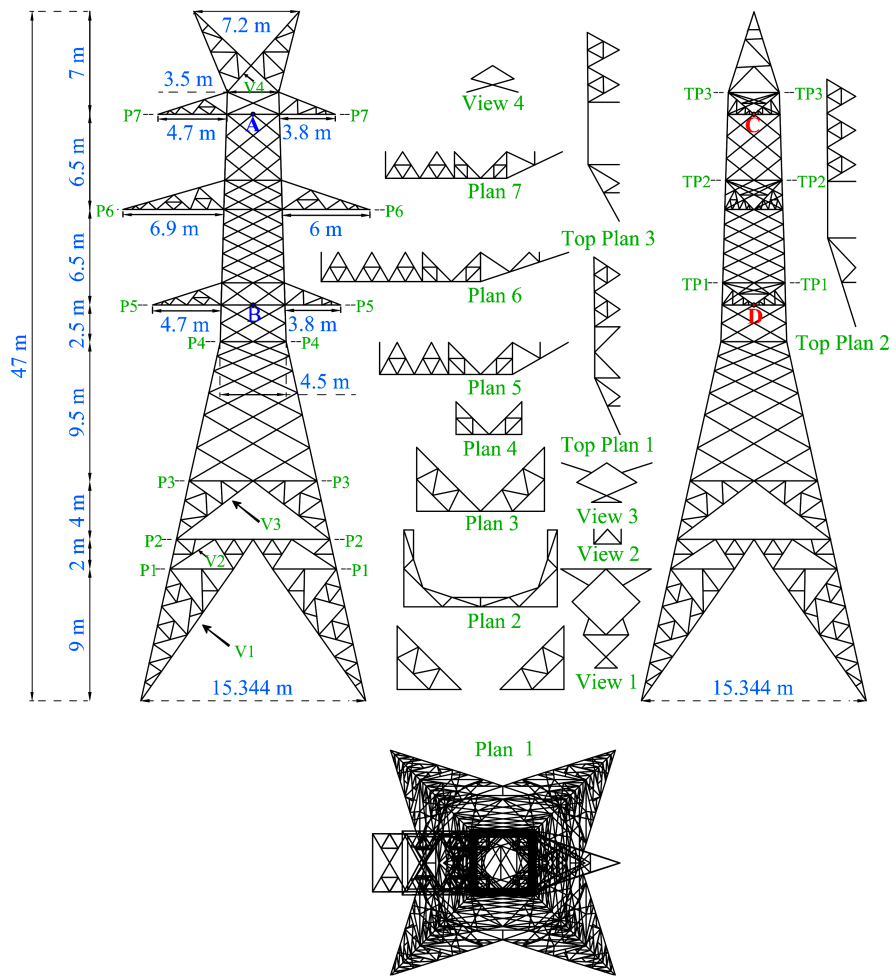


Figure 1. Tower's configuration and geometric dimensions.

of manual and automatic and the load can increase up to 40 tons using pulleys. Here, 30 lines of force are read continuously and simultaneously by load cells with 1% accuracy. Load cells are installed as close to the tower as possible for accurate and noise-free reading. Figure 2 presents a schematic view of the test setup and rigging of the tower. Figure 3 shows the values of forces in each load case applied to the tower during the test.

During the test, the tower loading was gradually applied in five steps: up to 50%, 75%, 90%, 95%, and 100% of the design forces, as shown in Figure 3, according to IEC60652 [43]. In the case of the tower failure at a load factor of less than 100%, the tower cannot pass the test, hence no longer acceptable. Given that a significant number of towers tested in the past experienced this failure during the test, the need for predicting the failure probability of tower in the type test for different load factors to reduce the design costs as well as build and retest the tower was highlighted. Load cases were employed to design the towers according to the relevant standards and applied to the tower exactly in the type test. The load values

for the studied tower in Figure 3 were determined based on the Iranian loading standard [44]. In this regard, H.W. (High Wind) load case was used for confirming the tower capacity for resisting high winds. Of note, the tower could pass the test without any failure. The load case BRS1C1 (Broken Wire Shield1 Cross Arm1) was also used to approve the tower capacity for resisting the rupture of cables at points S1 and C1 (Figure 4). In this case, due to the connection of other cables to the tower, the tower is subjected to unbalanced loading at the top. During the test, at 73% of the designing load, the bottom plate of the cross arm C1 failed (Figure 5(a)) and the test stopped mainly because the members' failure was equal to the tower failure.

After replacing the failed member with a stronger angle section, the tower was retested and the test continued up to 95% of the design load. At this time, the tower passed the test without any failure. The load case W.I. (Wind Ice) was utilized to confirm the tower capacity of resistance to the intense weather conditions. During the loading, cross arm C3 failed at 90% of the design load and the test stopped (Figure 5(b)).

After checking the tower at the end of the two



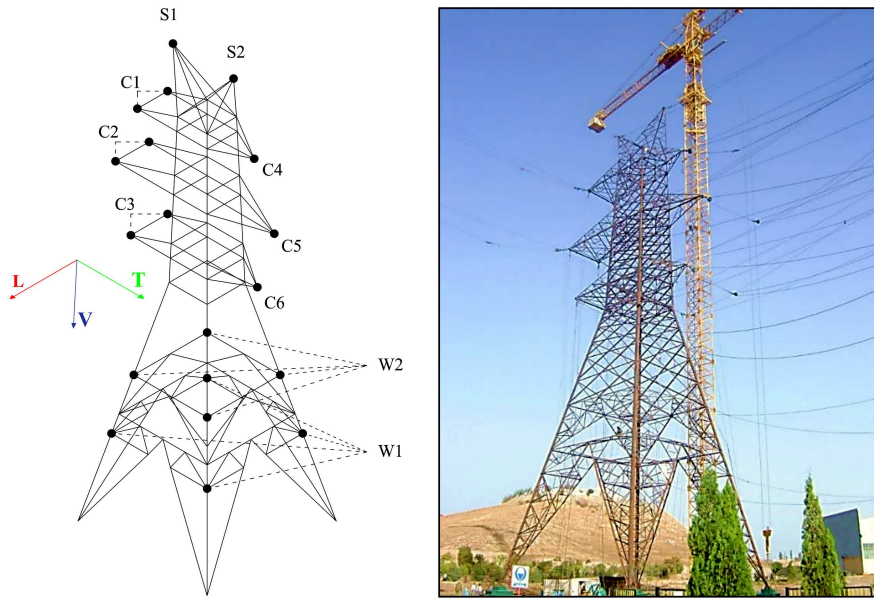


Figure 4. Loading points and tower's rigging for type test.



Figure 5. (a) Failure of the lower member of cross arm C1 under load case BRS1C1. (b) Failure of cross arm C3 under load case W.I.

6). In the same load case, one of the main members in the leg of the tower failed at the same time as the occurrence of the progressive failure of the cross arm C3 (Figure 6).

### 2.2. Development of the numerical model

In the numerical model, each member with an equal angle section was defined by the local coordinate system, as shown in Figure 7(a). The eccentricity value for all connections was chosen as 0.01 m. As observed in Figure 7(b), the unconnected side of a member is the side whose normal vector is the local  $y$ -axis. To consider the initial imperfection in members, a node was defined in the middle of every element with an extrusion obtained from dividing the length of the element by 500. Each part of a member with an equal angle section was modeled by the force-based

beam-column element in OpenSees. The eccentricity at two ends of the member was defined based on an elastic beam-column element with an elasticity modulus 100 times that of steel to behave rigidly. Corotational and linear geometry transformations were used for the major members and elements, respectively, which represent eccentricity. Six nonlinear springs at the terminal node of each member were defined by translational and rotational stiffness values along the local axes  $x$ ,  $y$ , and  $z$  using zero-length elements. Figure 7 shows three types of conventional bolted connections used in lattice transmission towers and their mechanical models in numerical model analysis. For instance, for the diagonal members connected to the leg bolted in one of their sides (Figure 7(d)), six nonlinear springs at the terminal node of each diagonal member were defined by transitional and

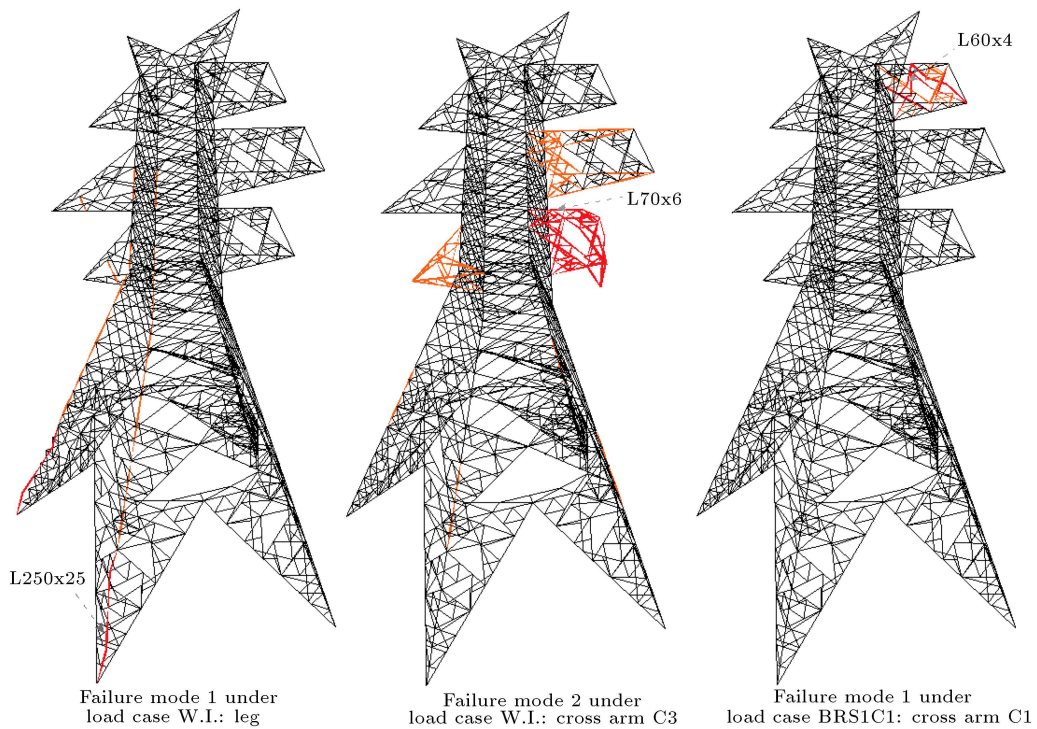


Figure 6. Areas prone to failure at the end of the tower test.

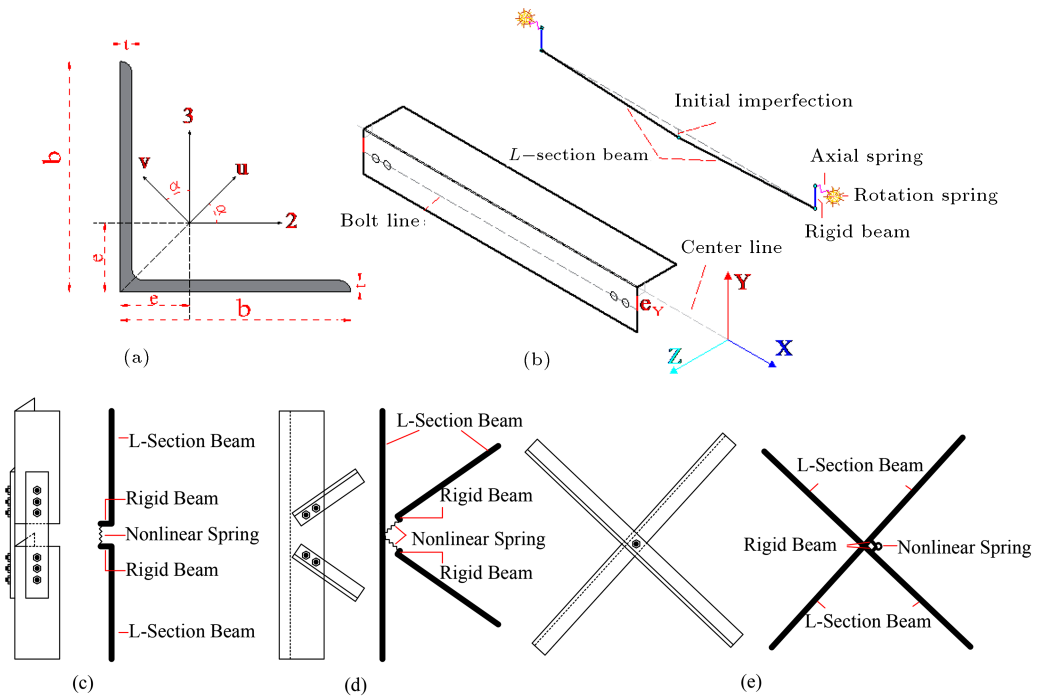


Figure 7. (a) The axes of the member. (b) Model details in OpenSees. (c) Members bolted together in their both sides. (d) Members bolted together in one side. (e) Members crossing over each other.

rotational stiffness values along the local axes  $x$ ,  $y$ , and  $z$  based on Zero Length Element. In OpenSees, Zero Length Element object is defined by two nodes in the same location [41]. Table 1 lists the stiffness values obtained from the study by Ungkurapinan et

al. [45] with parameters shown in Figure 8. They conducted laboratory studies to obtain more accurate models to examine joint slippage behavior. They also performed experiments on equal-angle sections where conventional bolt joints were connected by one or

**Table 1.** Characteristics of stiffness for bolted connections described in Figure 8.

Axial stiffness	A (kN)	B (kN)	C (kN)	D (kN)	E (kN)	K1 (kN/mm)	K2 (kN/mm)	K3 (kN/mm)	K4 (kN/mm)	T (mm)
Lap-splice bolted connection	43.28	$43.28 + 33.7 \times P^*$	216.4	285.15	299.68	263.45	20.99	43.65	86.55	0.36
Single-leg bolted connection	Number of bolts	A (kN)	Slope (kN/mm)		P (mm)		Q (mm)	B (kN)	R (mm)	C (kN)
	1	9.29	27.51				2.74	65.03	6.04	107.8
	2	20.14	84.81		P		1.73	91.51	2.55	157.7
	3	29.28	113.9				2.4	152.9	2.18	204.4
4	46.95	139				1.85	168.2	1.16	207.6	
Other stiffness values	Members bolted together		Number of bolts		$k_y$	$k_z$	$k_{rotx}$	$k_{roty}$	$k_{rotz}$	
	Single-leg		Single-bolt		Rigid	Rigid	Rigid	Rigid	Pinned	
	Single-leg		Two or more bolts		Rigid	Rigid	Rigid	Rigid	Rigid	
	Lap-splice		-		Rigid	Rigid	Rigid	Rigid	Rigid	

\*  $P \sim$  Uniform [0, 2.21] (mm)

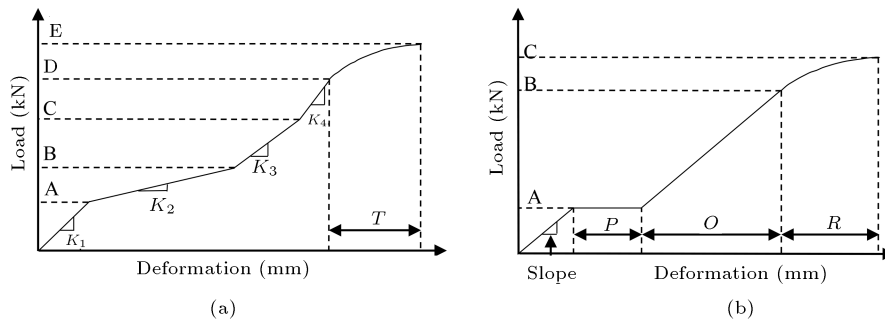


**Figure 8.** Modified joint slippage model proposed by Ungkurapinan et al. [45] for (a) Lap-splice bolted joint and (b) single-leg bolted joint.

both sides. Then, they developed mathematical and experimental equations to illustrate the slippage and force-displacement behavior (Figure 8). Elastic multi-linear material defines the stiffness of the spring in the  $x$ -direction in OpenSees. In addition, steel is modeled using Steel02 material with St 52 (DIN 2391) characteristics. Furthermore, the base supports are assumed rigid in the tower model.

**2.3. Model validation**

As mentioned earlier, the eccentricity and initial imperfection values of the developed model were set to 0.01 m and the member’s length was divided by 500. The modeled tower has 2358 members and each member is connected to the other ones at both ends with bolt connections; therefore, 4716 random variables are required to exactly define the eccentricity of connection among the members. To overcome this problem, eccentricity was considered as a random variable with a uniform distribution between 0 and 0.02 m. The value of 0 is perfectly centered to consider connections. Values greater than 0.02 m also made the amount of moment produced at both ends of the

member considerably high; consequently, the numerical model did not converge to the test results and failed earlier than the load coefficient recorded in the test. The eccentricity value in the model validation was set as the average value of the selected distribution. Jiang et al. [12] presented models with the maximum joint slippage (i.e., 0.00221 m) that followed the test results at the ultimate load values and they took into consideration the amount of joint slippage, which was considered a fixed value equal to 0.00221 m. One of the test outputs is the displacement record of points A, B, C, and D (see Figure 1) in every step of increasing load and for each load case. Force-control static pushover analysis was carried out to reach the maximum test load and in the final step, the displacements of the mentioned points were determined. Furthermore, for a better understanding of the effects of these parameters, the obtained results were compared with those from the simplified model where all connections were rigid and the members were centrally connected. Figures 9–11 present the comparative results for the test, developed model, and simplified model. According to Figures 9 and 10, the difference between the simplified model and

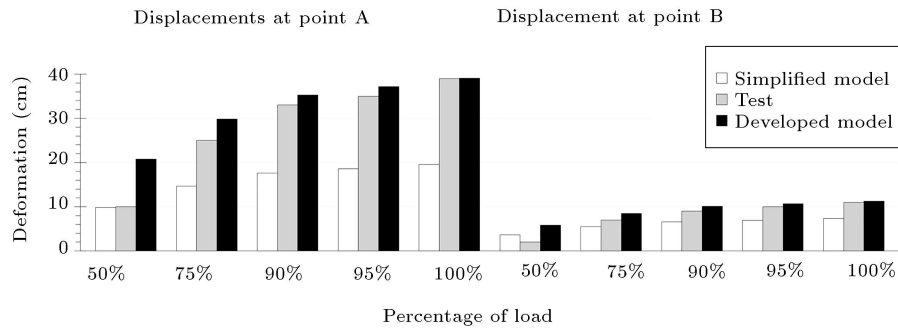


Figure 9. Comparison of displacements at points A and B in load case H.W.

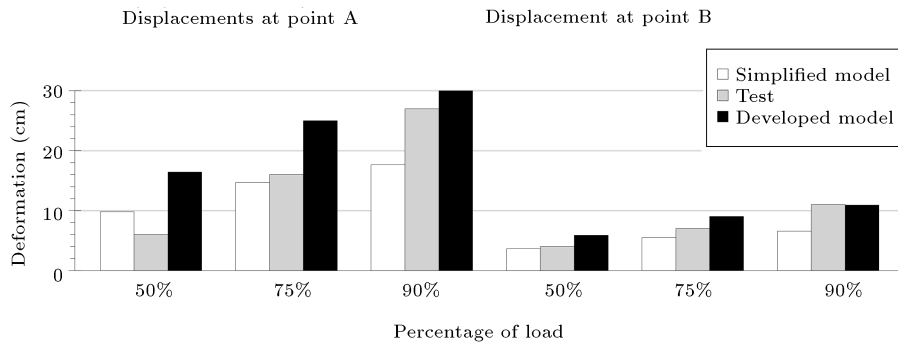


Figure 10. Comparison of displacements at points A and B in load case W.I.

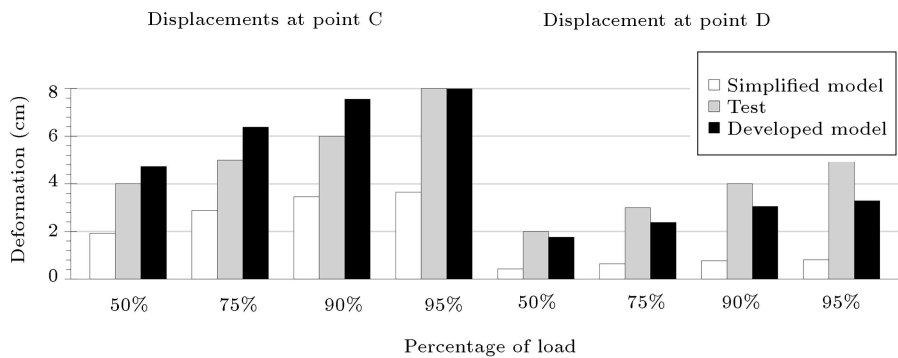


Figure 11. Comparison of displacements at points C and D in load case BRS1C1.

test results can reach up to 0.18 m under the H.W. load case and 0.09 m under the W.I. load case. As shown in Figures 9–11, the absolute error values at points A and B are 0.11 cm and 0.24 cm, respectively, in the load case H.W. and 3.33 cm and 0.057 cm, respectively, in load case W.I. Therefore, it can be concluded that the developed model can predict the displacement of the tower well in the longitudinal load cases. In the load case BRS1C1, the absolute error values at points C and D are 0.008 cm and 1.706 cm, respectively. In conclusion, the prediction results through the developed model agreed favorably with the test results. The maximum displacement of the tower under the transverse BRS1C1 load case in the test is 0.08 m. According to Figure 11, the difference between the simplified model and test results is 0.04 m.

Of note, the developed model can predict the maximum displacement of the tested tower under the BRS1C1 load case well.

### 3. Sensitivity analysis of the tower’s failure

#### 3.1. The importance vector measures derived by FOSM

The main objective in this step is to provide quantitative investigation into the reliability of the tower with respect to the LSFs based on tower displacement and the members’ forces, considering the random nature of variables involved in the model. For this purpose, the importance vectors derived from the reliability analysis using FOSM [42] were utilized. It was also assumed that there was no uncertainty in the amount of the

**Table 2.** Selected members for FOSM analysis in each load case.

Load case	Length (m)	$P_a$	Location	Cross-section of member
BRS1C1	1.072	$0.643 \times F_y$	Cross arm $C_1$	$L60 \times 4$
W.I failure mode 1	1.317	$0.967 \times F_y$	Leg	$L250 \times 25$
W.I failure mode 2	1.186	$0.601 \times F_y$	Cross arm $C_3$	$L70 \times 6$

loads applied to the tower in the type test. The eccentricity (Ecc) of all connections was regarded as a random variable with a uniform distribution between 0 and 0.02 m. The values greater than 0.02 m made the values of the moments at the two ends of the member so large that the loading could not be continued to the final step, which is contrary to the reported conditions of the test. The initial imperfection (*Imp*) in members was taken into account and a node was defined in the middle of every element with an extrusion obtained from dividing the length of the element using a random variable with a uniform distribution between 500 and 1000. The uncertainty of the initial state of connection before loading (i.e., joint slippage,  $P$ ) was defined as a random variable with a uniform distribution between 0 and 0.00221 m. The upper bound was finally chosen based on [46].

The eccentricity increases the moments at the member's ends. It is essential to use a function that can take into account the simultaneous effects of the axial force and bending around both principal axes of the equal angle section (Eq. (1)); this, in turn, considers the exceedance probability of the failure function as the member's failure probability [47].

$$g(\tilde{x}) = 1 - \left[ n^2 + m_v + \left( \frac{m_u}{1-n} \right)^2 \right], \quad (1)$$

where  $n = \frac{N}{N_p}$ ,  $m_u = \frac{M_u}{M_{up}}$ , and  $m_v = \frac{M_v}{M_{vp}}$  are the ratios of the applied loads ( $N$ ,  $M_u$ ,  $M_v$ ) to the maximum plastic capacities of the equal angle section. In addition,  $N_p$  is the plastic axial force capacity of the section, and  $M_{vp}$  and  $M_{up}$  are the plastic moment capacities around the weak and strong axes of the section, respectively (Figure 7(a)). Moreover,  $N$  refers to the axially applied force, and  $M_u$  and  $M_v$  are the decomposition of the moments around the strong and weak axes, respectively, based on Eqs. (2) and (3). In these equations,  $M_2$  and  $M_3$  are the moments around the local axis (Figure 7(a)).

$$M_u = M_2 \cos \alpha + M_3 \sin \alpha \stackrel{\alpha=45^\circ}{=} \frac{\sqrt{2}}{2} (M_2 + M_3), \quad (2)$$

$$M_v = -M_2 \sin \alpha + M_3 \cos \alpha \stackrel{\alpha=45^\circ}{=} \frac{\sqrt{2}}{2} (M_3 - M_2). \quad (3)$$

The LSF presented in Eq. (1) investigates the probability of the plastic joint formation in the members. Given that one of the reasons for failure is member's buckling, in order to investigate the probability of the members' buckling, the equations proposed in Section 3.6 of ASCE/SEI 10-15 [48] were employed to determine the maximum allowable axial force. Hence, the LSF can be altered based on Eq. (4):

$$g(\tilde{x}) = 1 - \left[ n'^2 + m_v + \left( \frac{m_u}{1-n'} \right)^2 \right], \quad (4)$$

where  $n' = \frac{N}{P_a A_g}$ ,  $m_u = \frac{M_u}{M_{up}}$ , and  $m_v = \frac{M_v}{M_{vp}}$  are the ratios of the applied loads to the maximum allowable axial force and maximum plastic capacities, respectively,  $P_a$  is the maximum allowable axial stress of the compression member according to ASCE 10-15 [48], and  $A_g$  is the section area.

The LSF of Eq. (4), which is more critical than that of Eq. (1), is evaluated by FOSM for the selected members listed in Table 2. These members are also shown in Figures 5 and 6. The FOSM importance measures for the mentioned random variables are presented in Table 3. In addition, displacement-based LSF is also considered in this study. Since the most significant displacement cases recorded during the test are related to the load case H.W. with 0.39 and 0.11 m on the target points A and B (see Figure 9), respectively, two implicit LSFs are defined and listed in Table 3 according to which the most significant variables for force- and displacement-based LSF are the eccentricity and joint slippage, respectively.

### 3.2. Proposed model for estimation of the additional moment due to the eccentricity

Based on the importance vectors of the variables in Table 3, it can be concluded that joint slippage, compared to other variables, has minor effect on the force-based LSF; therefore, it can be eliminated from the model for the sake of simplicity and computational time saving. The main members of the tower, according to Figure 4, are selected as the studied members and then, the tower is subjected to the load cases BRS1C1 and W.I. Then, the maximum axial force and moments around Axes 2 and 3 (Figure 7(a)) at each start, middle, and end of the member are recorded for different values of the

**Table 3.** Importance vector measures derived from FOSM analysis on the LSFs.

The evaluation state	Load case	Implicit LSF	Random variable	FOSM importance measure
Maximum load-carrying capacity	BRS1C <sub>1</sub>	Eq. (4)	<i>Ecc</i>	0.995
			<i>Imp</i>	0.093
			<i>P</i>	0.03
	W.I. failure mode 1	Eq. (4)	<i>Ecc</i>	0.999
			<i>Imp</i>	0.003
			<i>P</i>	0
W.I. failure mode 2	Eq. (4)	<i>Ecc</i>	0.864	
		<i>Imp</i>	0.505	
		<i>P</i>	0	
Displacements at the target points	H.W.	$g_A(\tilde{x}) = 0.39 - \text{Displacement}_A$	<i>P</i>	0.8
			<i>Ecc</i>	0.6
			<i>Imp</i>	0
	H.W.	$g_B(\tilde{x}) = 0.11 - \text{Displacement}_B$	<i>P</i>	0.71
			<i>Ecc</i>	0.7
			<i>Imp</i>	0

**Table 4.** Characteristics of the proposed linear regression model for  $M_i^*$ .

Linear regression model	Model parameter	Mean	CoV (%)	Model parameters correlation	R-factor	Mean of sigma	CoV of sigma (%)
$M_2^*$	$\theta_1$	5.198	0.428	0.680	0.945	0.683	0.603
	$\theta_2$	-0.104	0.308				
$M_3^*$	$\theta_1$	6.227	0.324	0.682	0.947	0.616	0.603
	$\theta_2$	-0.097	0.285				

eccentricity and initial imperfection. To account for the initial imperfection, the length of each element is divided into 500, 750, and 1000. The same values for the eccentricity are 0.0001, 0.005, 0.01, and 0.015. In this study, a total of 24 models were considered. The objective is to correlate the members' moments obtained from these models to those from a simplified model with no consideration of eccentricity and initial imperfection. To do so, the ordinary least square method [49] should be employed.

Modeling is an iterative process between error diagnosis and inference. A better model for the maximum output moments in the angular section in axes 2 and 3 (Figure 7(a)) can be obtained by removing the initial imperfection from the list of variables. The final

model is presented in Eq. (5). The initial imperfection variable was removed from the final form of Eq. (5) on condition that upon removing the initial imperfection variable from the final form of Eq. (5), no significant increase in the amount of  $\varepsilon$  (modeling error) would be observed. However, a penalty is given in Eq. (5) by removing the two variables of joint slippage and initial imperfection, showing its penalty in  $\varepsilon$ . The probabilistic characteristics of the equation parameters ( $\theta_1$  and  $\theta_2$ ) of the proposed model are listed in Table 4. The correlation between the equation parameters is 0.62. The correlation coefficient greater than 0.7 points to the independence of these two variables from each other [50]. A basic assumption about linear regression is that the errors are normally distributed; otherwise, it is a

sign of a model error [49]. The model error denoted by  $\varepsilon$  follows a normal distribution with the mean of zero. In the evaluated models, no difference was observed in the axial forces generated at both ends of the members. The proposed model is presented as follows:

$$Ln(M_i^*) = \theta_1 \frac{Ln(F)}{(LnEcc)^2} + \theta_2 Ln(Ecc) Ln(M_i) + \varepsilon$$

$i = 2,3$  The  $i$ th local axes (Figure 7(a)), (5)

where  $F$  (kg) is the maximum axial force in the model without eccentricity (obtained from the first-order analysis),  $Ecc$  (m) the eccentricity,  $M_i$  (kg.m) the maximum moment around the local axis in the model without eccentricity (obtained from the first-order analysis),  $\theta_1, \theta_2$  model parameters,  $\varepsilon$  the modeling error,  $i$  the  $i$ th local axes (Figure 7), and  $M_i^*$  (kg.m) the maximum moment around the local axis considering eccentricity (obtained from the second-order analysis).

**4. Results and discussion**

**4.1. Reliability analysis of the tower using FOSM, FORM, and SORM**

This section determines the failure probability of the tower in the type test under the specified load factor.

The random variables used for the reliability analysis of the tested tower include the eccentricity at the connections, modulus of elasticity, yield stress of the materials, and model errors from Table 5. Eccentricity plays an essential role in the model performance that should be taken into consideration since the results obtained from the simplified model (i.e., without eccentricity) in the case of the studied tower showed that the tower capacity could reach up to 1.15 times the design loads; however, the test results demonstrated that the tower capacity was about 0.9 times the design loads. To justify this difference up to the failure point, an eccentricity, probably related to how the tower members are assembled, should be considered in the connections. The eccentricity values at the design point of each LSF considered in every load case determine the value at which the investigated member would fail.

By performing FOSM analysis, First-Order Reliability Method (FORM), and Second-Order Reliability Method (SORM) by Breitung’s formula [51], the exceedance probability of the members listed in Table 2 is determined using the LSF considered in each load case. In Table 6, the failure probability of the selected members (Table 2) is calculated for two LSFs, namely plastic resistance (Eq. (1)) and buckling (Eq. (4)). A comparison of the failure probabilities revealed that the

**Table 5.** Introduction of the random variables used in reliability analysis.

Random variable	Variable symbol	Distribution	Mean	Std (CoV)	Units
Eccentricity	$Ecc$	Uniform	0.01	0.00572 (0.572)	m
Elastic modulus	$E$	Log-normal	$2.039E + 8$	2.039E+6 (0.01)	kN/m <sup>2</sup>
Yield strength	$F_y$	Log-normal	$3.6E + 5$	3.6E+3 (0.01)	kN/m <sup>2</sup>
$M_2^*$ model error	$\varepsilon_y$	Normal	0	0.68301	–
$M_3^*$ model error	$\varepsilon_z$	Normal	0	0.6162	–

**Table 6.** Results of reliability analyses.

	Load case	BRS1C1	W.I. failure mode 1	W.I. failure mode 2	BRS1C1	W.I. failure mode 1	W.I. failure mode 2
		Eq. (1)	Eq. (1)	Eq. (1)	Eq. (4)	Eq. (4)	Eq. (4)
Implicit limit state							
FOSM analysis	FOSM $\beta$	6.3	8.45	2.83	2.72	7.4	0.86
	Failure probability (in percentage)	1.49e-8	1.46e-15	0.23	0.33	6.81e-12	19.49
FORM analysis	FORM $\beta$	1.89	2.025	1.25	1.098	1.88	0.53
	Failure probability (in percentage)	2.93	2.14	10.65	13.6	3.01	29.76
SORM analysis	SORM $\beta$	1.2	2.16	1.36	1.21	1.9	0.37
	Failure probability (in percentage)	11.53	1.52	8.76	11.29	2.8 8	35.50

higher failure probability values (i.e., lower  $\beta$  values) were attributed to the LSF concerning buckling. In FORM analysis, the failure probability of buckling is greater than that of plastic strength up to 19% in the critical members under W.I. load case. In addition, a comparison of the  $\beta$  values obtained from different reliability methods indicated that FOSM yielded the least value of failure probabilities, while FORM and SORM methods provided a much higher estimation of the failure probability.

**4.2. Fragility curves of the tower**

Figure 12 presents the fragility curves that express the failure probability of the tested tower in the load cases against the load factors. In fact, the current study primarily aims to introduce, classify, and implement random variables involved in constructing and modeling the fragility curves of the tested tower. Upon estimating the fragility curves in the members whose failure was observed during the tower test, the force-based LSF was used to evaluate the probability of failure through the FORM method. To be specific, the corresponding failure probability was estimated for a set of load factors. While estimating the failure probability based on the FORM method, the point on the surface with the lowest beta (design point) was also determined. The properties of the lognormal function fitted to the fragility curves are shown in Figure 12. In this figure, the eccentricity calculated at the designing point is also given a value for which the tower can fail

with a certain probability. The flowchart summarizing all the steps used to produce the fragility curve is depicted in Figure 13. Figure 12 demonstrates that the second-order effects created by the bolted connections can be large enough to make the main members fail. For instance, in load pattern W.I. (failure mode 2) and a load factor of 0.8, an eccentricity of about 0.014 m at the connections can increase the failure probability of the tower up to 18%, which is significant (see Figure 12). Besides, at the lower load factors, a higher eccentricity may cause the tower failure. Based on the slope of the eccentricity curves in Figure 12, it is concluded that at load factors greater than about 0.8, the impact of eccentricity on the tower failure becomes significant. This is important in the sense that the tower failure occurs most likely at the load factors in the range of 0.8–1. The information provided in Figure 12 is used to analyze the failure of the tested tower. Based on the test results, the tower failed at the bottom plate of cross arm C3 in load case W.I. and at 90% of the designing load. According to Figure 12, the failure probabilities in the leg and the cross arm at the load factor of 0.9 are estimated as 3% and 30%, respectively. Thus, the tower is more susceptible to failure in the cross arm rather than the leg, which is verified by the type test in which the tower’s failure starts from this area. It is also noted that the eccentricities associated with the leg and cross arm failure modes are determined as 0.015 and 0.013 m, respectively (Figure 12). It is also seen that W.I. (failure mode 2) is more critical

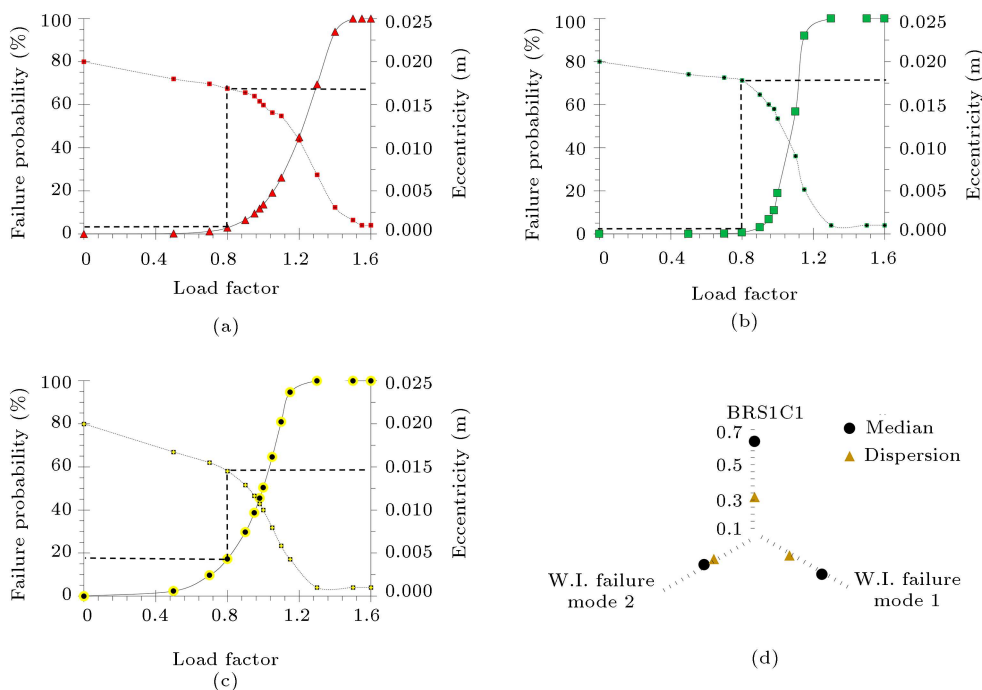


**Figure 12.** Tower’s fragility curve and corresponding eccentricity in (a) Load case BRS1C1, (b) load case W.I. failure mode 1, (c) load case W.I. failure mode 2, and (d) lognormal parameters for the fragility of the tested tower.

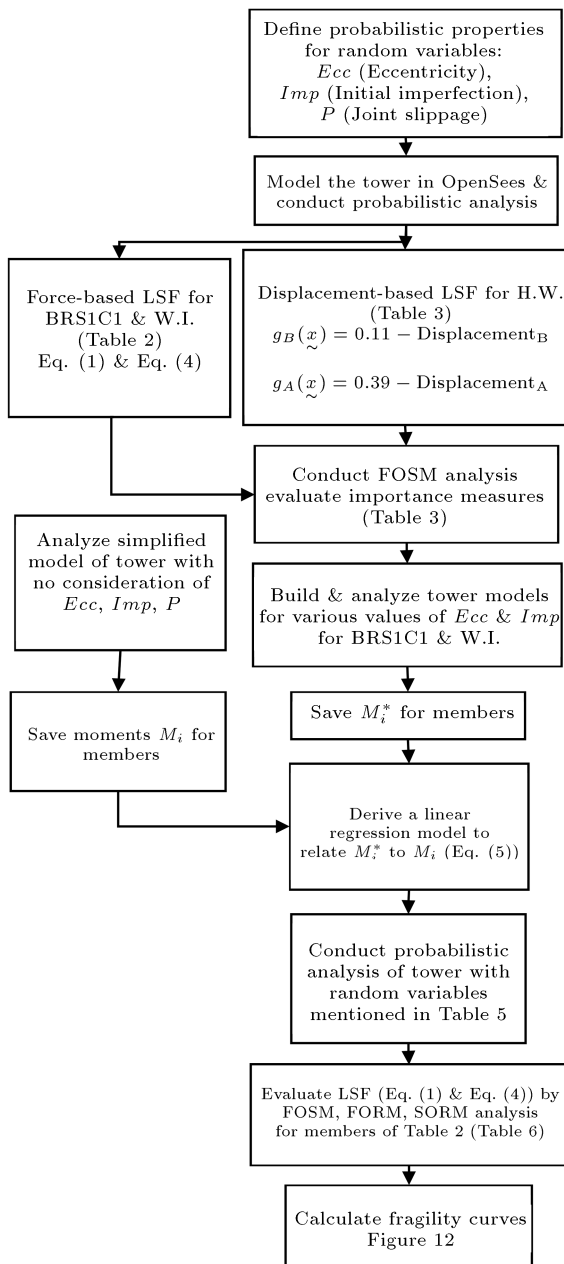


Figure 13. Flowchart for development of fragility curves.

than BRS1C1 since the fragility curve of the former stands higher than that of the latter in Figure 12. This is in agreement with the test observations.

## 5. Conclusions

The current study developed a probabilistic framework to analyze the failure of a transmission tower in a full-scale type test, taking into account the random nature of uncertainties inherent in eccentricities of connections, initial imperfections of members, joint slippage, and mechanical properties of steel. To this end, a finite element model of the tower was developed and verified by the test results. In order to account

for the eccentricities, a regression-based equation was proposed to obtain the surplus bending in the members from a simplified finite element model of the tower. The utilized Limit State Functions (LSFs) based on both displacement and resistance were evaluated through different reliability techniques. In addition, the failure probability at different load factors was presented in terms of fragility curves for different load patterns. The main findings of this study are summarized below:

1. Incorporation of joint slippage into the model is essential to accurate estimation of the tested tower displacement. Regardless of joint slippage, the difference between the model and test results reached up to 0.18 meters under the H.W. load case;
2. The importance vector measures derived from First Order Second Moment (FOSM) analysis indicated that eccentricity and joint slippage were considered the most critical force-dependent variable and the most significant displacement-dependent variable, respectively;
3. For comparing the failure probabilities of the tower members based on First-Order Reliability Method (FORM) analysis under limit states related to plastic versus buckling capacities, it was observed that the amount of failure probability resulting from buckling was larger up to 19% in the critical members under the W.I. load case;
4. The reliability analysis in this study could predict the failure mode of the tower in the type test. The calculated failure probabilities for cross arm and leg under the W.I. load case were 30% and 3% at a load factor of 0.9, respectively, indicating that the tower was more susceptible to failure in the cross arm rather than the leg, as verified by the test results;
5. The failure probability of the tower against different load factors (i.e., the fragility curve) was also determined in this study. Moreover, the eccentricities associated with the failure at different load factors were calculated. According to the findings, at load factors greater than 0.8, the impact of eccentricity on the tower failure was significant.

As a future research suggestion, the reliability-based method of failure analysis developed in this paper can be applied to other types of towers with different load patterns and failure modes.

## Nomenclature

$A_g$	Section area
BRS1C1	Broken Wire Shield1 Cross Arm1 load case
Dispersion	Lognormal parameters for the fragility of the tested tower

Developed model	Considering eccentricity, initial imperfection, and joint slippage in modeling
$Ecc$	The eccentricity of connection
FOSM	First Order Second Moment
FORM	First Order Reliability Method
$F_y$	Yield stress
$F$	Maximum axial force in the model without eccentricity (obtained from the first-order analysis)
$H.W.$	High Wind load case
$i$	The $i$ th local axes (Figure 7(a))
$Imp$	Initial imperfection
LSF	Limit State Function
$LN(\mu, \sigma)$	Lognormal distribution with mean $\mu$ and standard deviation $\sigma$
$M_{up}, M_{vp}$	Section's plastic moment capacity around the strong and weak axes, respectively (Figure 7(a))
$M_u, M_v$	Decomposition of the moments around the strong and weak axes, respectively
$M_i$	The maximum moment around the local axis (Figure 7(a)) in the model without eccentricity (obtained from the first-order analysis)
$M_i^*$	The maximum moment around the local axis in the fiber model considering eccentricity (obtained from the second-order analysis)
$m_v = \frac{M_v}{M_{vp}}$	Ratios of the applied loads to the
$m_u = \frac{M_u}{M_{up}}$	Maximum plastic capacities
Mean	The mean of distribution
Median	Lognormal parameters for the fragility of the tested tower
$N_p$	Section's plastic axial force capacity
$n = \frac{N}{N_p}$	Ratios of the applied loads to the maximum plastic capacities
$n' = \frac{N}{P_a A_g}$	The ratio of the axial force applied to the member to its maximum allowable axial force
$N(\mu, \sigma)$	Normal distribution with mean $\mu$ and standard deviation $\sigma$
$P$	Joint slippage
$P_a$	The maximum allowable axial stress of the compression member according to ASCE 10-15
SORM	Second Order Reliability Method
Std	Standard deviation of distribution

Simplified model	All connections being rigid and the members centrally connected
$U(a,b)$	Uniform distribution between $a$ and $b$
W.I	Wind Ice load case

### Greek symbols

$\theta_1, \theta_2$	Model parameters
$\beta$	Reliability index
$\varepsilon$	Modeling error

### References

- Paiva, F., Henriques, J., and Barros, R.C. "Review of transmission tower testing stations around the world", *Procedia Engineering*, **57**, pp. 859–868 (2013).
- Rao, N.P., Mohan, S.J., and Lakshmanan, N. "A study on failure of cross arms in transmission line towers during prototype testing", *International Journal of Structural Stability and Dynamics*, **05**(03), pp. 435–455 (2005).
- Tian, L., Guo, L., Ma, R., et al. "Full-scale tests and numerical simulations of failure mechanism of power transmission towers", *International Journal of Structural Stability and Dynamics*, **18**(09), p. 1850109 (2018).
- Shukla, V.K. and Selvaraj, M. "Assessment of structural behavior of transmission line tower using strain gauging method", *International Journal of Steel Structures*, **17**(4), pp. 1529–1536 (2017).
- Tian, L., Pan, H., Ma, R., et al. "Full-scale test and numerical failure analysis of a latticed steel tubular transmission tower", *Engineering Structures*, **208**(October), p. 109919 (2020).
- Prasad Rao, N., Knight, G.M.S., Lakshmanan, N., et al. "Investigation of transmission line tower failures", *Engineering Failure Analysis*, **17**(5), pp. 1127–1141 (2010).
- Lu, C., Ma, X., and Mills, J.E. "Modeling of retrofitted steel transmission towers", *Journal of Constructional Steel Research*, **112**, pp. 138–154 (2015).
- Albermani, F., Kitipornchai, S., and Chan, R.W.K. "Failure analysis of transmission towers", *Engineering Failure Analysis*, **16**(6), pp. 1922–1928 (2009).
- de Souza, R.R., Fadel Miguel, L.F., Kaminski, J., et al. "Topology design recommendations of transmission line towers to minimize the bolt slippage effect", *Engineering Structures*, **178**(August 2018), pp. 286–297 (2019).
- Jiang, W.Q., Wang, Z.Q., McClure, G., et al. "Accurate modeling of joint effects in lattice transmission towers", *Engineering Structures*, **33**(5), pp. 1817–1827 (2011).
- Albermani, F.G.A. and Kitipornchai, S. "Numerical simulation of structural behaviour of transmission towers", *Thin-Walled Structures*, **41**(2–3), pp. 167–177 (2003).

12. Wen-qiang, J., Zhang-qi, W., and McClure, G. "Notice of retraction: Failure analysis of lattice transmission tower considering joint effects", *2010 International Conference on Computer Application and System Modeling (ICCASM 2010)*, IEEE, pp. V5-602-V5-605 (2010).
13. Szafran, J. and Rykaluk, K. "Steel lattice tower under ultimate load-chosen joint analysis", *Civil and Environmental Engineering Reports*, **25**(2), pp. 199–210 (2017).
14. Yaghoobi, S. and Shooshtari, A. "Joint slip investigation based on finite element modelling verified by experimental results on wind turbine lattice towers", *Frontiers of Structural and Civil Engineering*, **12**(3), pp. 341–351 (2018).
15. An, L., Wu, J., and Jiang, W. "Experimental and numerical study of the axial stiffness of bolted joints in steel lattice transmission tower legs", *Engineering Structures*, **187**(March), pp. 490–503 (2019).
16. Ungkurapinan, N., Chandrakeerthy, S.R.D.R.D.S., Rajapakse, R.K.N.K.N.D., et al. "Joint slip in steel electric transmission towers", *Engineering Structures*, **25**(6), pp. 779–788 (2003).
17. Ahmed, K.I.E., Rajapakse, R.K.N.D., and Gadala, M.S. "Influence of bolted-joint slippage on the response of transmission towers subjected to frost-heave", *Advances in Structural Engineering*, **12**(1), pp. 1–17 (2009).
18. Kitipornchai, S., Al-Bermani, F.G.A., and Peyrot, A.H. "Effect of bolt slippage on ultimate behavior of lattice structures", *Journal of Structural Engineering*, **120**(8), pp. 2281–2287 (1994).
19. Temple, M.C., Sakla, S.S.S., Stchyrba, D., et al. "Arrangement of interconnectors for starred angle compression members", *Canadian Journal of Civil Engineering*, **21**(1), pp. 76–80 (1994).
20. Hoseini, S.A., Ghaemian, M., and Hariri-Ardebili, M.A. "Uncertainty quantification in seismic collapse assessment of the Iranian code-conforming RC buildings", *Scientia Iranica*, **27**(4), pp. 1786–1802 (2020).
21. Fong, M., Cho, S.-H., and Chan, S.-L. "Design of angle trusses by codes and second-order analysis with experimental verification", *Journal of Constructional Steel Research*, **65**(12), pp. 2140–2147 (2009).
22. Fu, X., Wang, J., Li, H.-N., et al. "Full-scale test and its numerical simulation of a transmission tower under extreme wind loads", *Journal of Wind Engineering and Industrial Aerodynamics*, **190** (November 2018), pp. 119–133 (2019).
23. Tian, L., Pan, H., and Ma, R. "Probabilistic seismic demand model and fragility analysis of transmission tower subjected to near-field ground motions", *Journal of Constructional Steel Research*, **156**, pp. 266–275 (2019).
24. Da Silva, J.G.S., Vellasco, P.C.G.D.S., De Andrade, S.A.L., et al. "Structural assessment of current steel design models for transmission and telecommunication towers", *Journal of Constructional Steel Research*, **61**(8), pp. 1108–1134 (2005).
25. Lee, P.-S. and McClure, G. "Elastoplastic large deformation analysis of a lattice steel tower structure and comparison with full-scale tests", *Journal of Constructional Steel Research*, **63**(5), pp. 709–717 (2007).
26. Prasad Rao, N. and Kalyanaraman, V. "Non-linear behaviour of lattice panel of angle towers", *Journal of Constructional Steel Research*, **57**(12), pp. 1337–1357 (2001).
27. Zhuge, Y., Mills, J.E., and Ma, X. "Modelling of steel lattice tower angle legs reinforced for increased load capacity", *Engineering Structures*, **43**, pp. 160–168 (2012).
28. Fu, X. and Li, H.-N. "Uncertainty analysis of the strength capacity and failure path for a transmission tower under a wind load", *Journal of Wind Engineering and Industrial Aerodynamics*, **173**(February), pp. 147–155 (2018).
29. Mohammadi Darestani, Y., Shafieezadeh, A., and Cha, K. "Effect of modelling complexities on extreme wind hazard performance of steel lattice transmission towers", *Structure and Infrastructure Engineering*, **16**(6), pp. 898–915 (2020).
30. Fu, X., Li, H.N., and Wang, J. "Failure analysis of a transmission tower subjected to combined wind and rainfall excitations", *Structural Design of Tall and Special Buildings*, **28**(10), pp. 1–19 (2019).
31. Tessari, R.K., Kroetz, H.M., and Beck, A.T. "Performance-based design of steel towers subject to wind action", *Engineering Structures*, **143**, pp. 549–557 (2017).
32. Pan, H., Tian, L., Fu, X., et al. "Sensitivities of the seismic response and fragility estimate of a transmission tower to structural and ground motion uncertainties", *Journal of Constructional Steel Research*, **167**, p. 105941 (2020).
33. Fu, X., Wang, J., and Li, H. "Failure analysis of a transmission tower induced by wind loads", *The 2018 Structures Congress (Structures18)*, Songdo Convention, Incheon, Korea (2018).
34. Sotoudeh, M.A., Ghaemian, M., and Moghadam, A.S. "Determination of limit-states for near-fault seismic fragility assessment of concrete gravity dams", *Scientia Iranica*, **26**(3A), pp. 1135–1155 (2019).
35. Li, X., Zhang, W., Niu, H., et al. "Probabilistic capacity assessment of single circuit transmission tower-line system subjected to strong winds", *Engineering Structures*, **175**(July), pp. 517–530 (2018).
36. Liu, Y., Lu, N., Yin, X., et al. "An adaptive support vector regression method for structural system reliability assessment and its application to a cable-stayed bridge", *Proceedings of the Institution of Mechanical Engineers, Part O: Journal of Risk and Reliability*, **230**(2), pp. 204–219 (2016).

37. Shafaei, A., Gholami, A., and Shariatinasab, R. “Probabilistic evaluation of lightning performance of overhead transmission lines, considering non-vertical strokes”, *Scientia Iranica*, **19**(3), pp. 812–819 (2012).
38. Szafran, J., Juszczak, K., and Kamiński, M. “Experiment-based reliability analysis of structural joints in a steel lattice tower”, *Journal of Constructional Steel Research*, **154**, pp. 278–292 (2019).
39. Liu, Z. and Feng, X. “A real-time reliable condition assessment system for 500 kV transmission towers based on stress measurement”, *Mathematical Problems in Engineering*, **2019**, pp. 1–8 (2019).
40. Szafran, J., Juszczak, K., and Kamiński, M. “Reliability assessment of steel lattice tower subjected to random wind load by the stochastic finite-element method”, *ASCE-ASME Journal of Risk and Uncertainty in Engineering Systems, Part A: Civil Engineering*, **6**(1), p. 04020003 (2020).
41. McKenna, F., Fenves, G.L., and Scott, M. H. “Open system for earthquake engineering simulation”, *Pacific Earthquake Engineering Research Center* (2000).
42. Mahsuli, M. and Haukaas, T. “Computer program for multimodel reliability and optimization analysis”, *Journal of Computing in Civil Engineering*, **27**(1), pp. 87–98 (2013).
43. IEC 60652, Loading tests on overhead line structures (2002).
44. Tavanir, *Codes and Standards for Loading Transmission Line Towers*, Tehran (1998).
45. Ungkurapinan, N., Chandrakeerthy, S.R.D.S., Rajapakse, R.K.N., et al. “Joint slip in steel electric transmission towers”, *Engineering Structures*, **25**(6), pp. 779–788 (2003).
46. Ungkurapinan, N., Chandrakeerthy, S.R.D.S., Rajapakse, R.K.N.D., et al. “Joint slip in steel electric transmission towers”, *Engineering Structures*, **25**(6), pp. 779–788 (2003).
47. Charalampakis, A. “Full plastic capacity of equal angle sections under biaxial bending and normal force”, *Engineering Structures*, **33**(6), pp. 2085–2090 (2011).
48. ASCE, *Design of Latticed Steel Transmission Structures*, ASCE 10-15 (2015).
49. Bishop, C.M., *Pattern Recognition and Machine Learning*, Springer, New York (2006).
50. Haldar, A. and Mahadevan, S. *Probability, Reliability and Statistical Method in Engineering Design* (2000).
51. Der Kiureghian, A. “First- and second-order reliability methods”, In *Engineering Design Reliability Handbook*, CRC Press (2006).

## Biographies

**Amir Mahmoudi** received the BSc degree in Civil Engineering from the Amirkabir University of Technology, Tehran, Iran, in 2017 and MSc degree in Structural Engineering from K. N. Toosi University of Technology, Tehran, Iran in 2020. In 2017, he received a scholarship from the Ministry of Energy - Niroo Research Institute in the form of a joint thesis with K. N. Toosi University of Technology. His research interest areas include reliability analysis, risk assessment, direct and indirect loss estimation in the power industry, machine learning, and programming, especially Python.

**Mohammad-Ali Jafari** was born in Tehran in 1974. He received the BS and MS degrees in Civil and Structural Engineering from the Sharif University of Technology in Tehran, Iran in 1999 and 2002, respectively, and the PhD degree in Earthquake engineering from IIEES, Tehran in 2009. Since 2009, he has been an Assistant Professor at the Power Industry Structures Research Department at Niroo Research Institute (NRI) in Tehran City. He is the author of more than 37 articles. He has participated in more than 17 research projects. His research interests include structural reliability, statistical modeling, and earthquake engineering, especially in electric power structures.

**Kourosh Nasrollahzadeh** is an Assistant Professor in Structural Engineering at the Department of Civil Engineering at K. N. Toosi University of Technology in Tehran, Iran. He received the Japan Concrete Institute (JCI) award for outstanding paper and presentation in two successive years in 2001 and 2002. He was awarded a post-doctoral research fellowship at the University of Tokyo in Japan in 2004–2006. His research interests include seismic retrofitting of structures by FRP, experimental research, and reliability analysis.